WATER RESOURCES RESEARCH, VOL. 24, NO. 2, PAGES 239–246, FEBRUARY 1988

The Fluid Mechanics of Fracture and Other Junctions

J. R. PHILIP

Division of Environmental Mechanics, CSIRO, Canberra, ACT, Australia

In connection with solute transfer in fracture networks, Hull and Koslow (1986) proposed proportional routing of streamlines through discontinuous fracture junctions (in which inlet and outlet branches alternate). We apply fluid mechanics to the problem and show that the errors of proportional routing may be unacceptably large when the two inlet discharges and the two outlet discharges both differ greatly in magnitude. In extreme cases one inlet flow is wholly excluded from one of the two outlets, and proportional routing is maximally incorrect. Solutions are established for arbitrary discharge patterns through four-way coplanar junctions: exact solutions for Laplace flows (Hele-Shaw flows and Darcy flows (fractures filled with porous material)) and approximate solutions for Stokes flows. The Laplace solutions apply also to a range of transport processes.

1. INTRODUCTION

This communication was stimulated by a recent treatment of streamline routing through fracture junctions [*Hull and Koslow*, 1986]. These authors recognized that the assumption of complete mixing at junctions may be unrealistic and that streamline routing is needed for the proper treatment of solute transport in fracture networks.

They studied a model junction with four equal, coplanar branches meeting at right angles, with two inlets and two outlets. They noted that the (gross) streamline routing problem is obvious and unambiguous for (in their parlance) "continuous" junctions, but is not so clear for "discontinuous" ones. Their continuous junctions have the two inlets (and the two outlets) adjacent, whereas the discontinuous ones have inlets and outlets alternating. After some qualitative discussion, they arrived at a method of routing through discontinuous junctions in which each inlet flow is distributed to the outlets in proportion to the two outlet flows. We shall call this method proportional routing. Paradoxically, it gives results equivalent to the complete mixing assumption, which *Hull and Koslow* [1986] questioned.

Hull and Koslow [1986] eschewed the application of quantitative fluid mechanics. Here we report an exploratory fluid mechanical study of their problem.

Our analysis depends on the same physical assumptions as those of *Hull and Koslow* [1986], namely, (1) flows are steady and for small Reynolds number; (2) within the junction solute diffusion across the dividing streamline is negligible; and (3) the treatment concerns mean solute concentration in each branch, which is also the uniform concentration in the branch far enough from the junction; in outlet branches this uniformity is achieved through diffusion within the branch.

2. KINEMATICS OF DISCONTINUOUS JUNCTIONS

Figure 1 shows the junction arrangement. We adopt rectangular Cartesian coordinates (x, y), and without loss of generality, we take the square $|x| \le 1$, $|y| \le 1$ as the junction, and branches 1, 2, 3, and 4 as

$$x > 1 \quad |y| \le 1 \qquad |x| \le 1, \quad y > 1$$

$$x < -1, \quad |y| \le 1 \qquad |x| \le 1, \quad y < -1$$

Paper number 7W4836.
0043-1397/88/007W-4836$05.00

respectively. The branch numbers are in counterclockwise order, different from the numbering scheme of *Hull and Koslow* [1986]. Let Q_i be the discharge in branch i, flow into the junction being taken positive. Then continuity requires that

$$\sum_i Q_i = 0 \tag{1}$$

With no loss of generality we take directions x, y such that for discontinuous junctions,

$$Q_2 \ge Q_4 > 0 \qquad Q_3 \le Q_1 < 0 \tag{2}$$

In view of (1) a triad of numbers specifies the branch discharges. It is convenient to take these as (Ω, X, Y) defined by

$$\begin{aligned} \Omega &= -\tfrac{1}{2}(Q_1 + Q_3) = \tfrac{1}{2}(Q_2 + Q_4) \\ X &= \tfrac{1}{2}(Q_1 - Q_3) \\ Y &= \tfrac{1}{2}(Q_2 - Q_4) \end{aligned} \tag{3}$$

It follows from (2) and (3) that

$$\begin{aligned} Q_1 &= -\Omega + X < 0 \qquad Q_2 = \Omega + Y > 0 \\ Q_3 &= -\Omega - X < 0 \qquad Q_4 = \Omega - Y > 0 \\ \Omega &> X \ge 0 \qquad \Omega > Y \ge 0 \end{aligned} \tag{4}$$

Normalizing discharges with respect to Ω, we finally write

$$a = X/\Omega \qquad b = Y/\Omega \tag{5}$$

with $0 \le a < 1$, $0 \le b < 1$. Then the normalized triad $(1, a, b)$ specifies the full range of possible discontinuous discharge patterns through the junction of Figure 1.

3. FLUID MECHANICS

Hull and Koslow [1986] state that the branches of their experimental model were "0.16 cm wide and 0.95 cm deep," i.e., L, the dimension normal to the (x, y) plane, was about 6 times that in the plane. The flow thus approximates a Stokes flow [*Stokes*, 1851] in the plane, satisfying the equation

$$\nabla^4 \Phi = 0 \tag{6}$$

with Φ the stream function defined by the relations

$$Lu = \partial\Phi/\partial y \qquad Lv = -\partial\Phi/\partial x \tag{7}$$

Here u is the component of flow velocity in the x direction (averaged normal to the (x, y) plane) and v that in the y

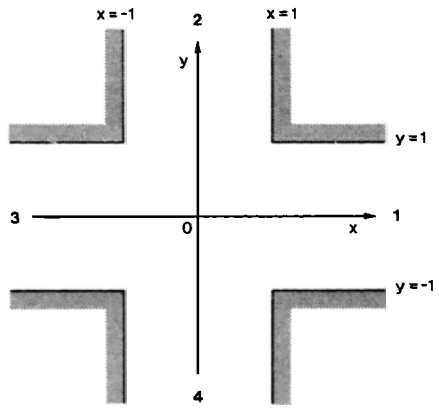

Fig. 1. Model junction showing coordinates and branch numbers.

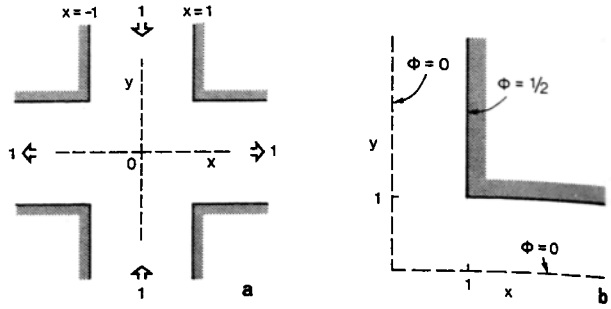

Fig. 2. (*a*) Discharge pattern (1, 0, 0). (*b*) Boundary conditions for the upper right quadrant.

direction. For Stokes flow the velocity distribution across each branch tends to be parabolic far from the junction and still close to parabolic nearer the junction. We shall here also examine what we shall call Laplace flows. These (mathematically simpler) Laplace flows are approximated when L is small compared with the branch dimension in the (x, y) plane, so that the system becomes a Hele-Shaw cell [*Hele-Shaw*, 1898]. A second situation producing Laplace flows may occur when the branches and the junction are filled with porous material. The flow system may then behave as a saturated homogeneous isotropic porous medium obeying Darcy's Law. In both circumstances the flow equation becomes Laplace's equation

$$\nabla^2\Phi = 0 \tag{8}$$

with Φ again defined by (7). Note that in wider contexts, not only Hele-Shaw and Darcy flows obey (8) but so also do potential (inviscid irrotational incompressible) flows and many other transport processes. Results below for Laplace flows thus apply to streamline routing for the wide range of flows described by (8).

We first study streamline routing through discontinuous junctions for flow satisfying (8). We then go on to give approximate results for the more difficult problem of flows satisfying (6). The Laplace (8) solutions apply when branch aspect ratio (depth/width) is small, and the Stokes solutions apply when it is large. The two sets of solutions thus set bounds on possible junction behavior.

4. Laplace Flows

4.1. *Decomposing the Problem*

The linearity of (8) (and later equation (6)), together with our normalized triadic specification of the discharges and symmetry considerations, enables us to construct solutions for all discharge patterns from two simple canonical solutions.

4.2. *Discharge Pattern (1, 0, 0)*

The first is for the pattern (1, 0, 0), illustrated in Figure 2*a*. The symmetry implies that we need solve (8) only in the quadrant $x \geq 0$, $y \geq 0$ subject to the boundary conditions

$$\begin{aligned} \Phi &= 0 \quad \text{on } x = 0 \quad y = 0 \\ \Phi &= \tfrac{1}{2} \quad \text{on } x = 1,\ y \geq 1 \quad x \geq 1,\ y = 1 \end{aligned} \tag{9}$$

(See Figure 2*b*.) (Strictly, we need solve only in the octant $y \geq x \geq 0$, but it proves convenient to work with the whole quadrant.)

The required solution, found in implicit form by conformal mapping (appendix), gives the coordinates $x(r)$, $y(r)$ of the streamline Φ, with the parameter r ranging from 0 as $y \to \infty$ to ∞ as $x \to \infty$. It is

$$x = x_1 + \pi^{-1} \cosh^{-1}\left[\frac{\cosh \pi y_1}{r}\right] \tag{10a}$$

$$y = y_1 + \pi^{-1} \cos^{-1}\left[\frac{\cos \pi x_1}{r}\right] \tag{10b}$$

$$x_1 = \pi^{-1} \cos^{-1} \pm\left[\frac{1 + r^2 - [(1 + r^2)^2 - 4r^2 \cos^2 2\pi\Phi]^{1/2}}{2}\right]^{1/2} \tag{10c}$$

$$y_1 = \pi^{-1} \cosh^{-1}\left[\frac{r \cos 2\pi\Phi}{\cos x_1}\right] \tag{10d}$$

The sign $\pm$ is taken according to the sign of $\cos 2\pi\Phi$. We denote the explicit form of solution (10) by $F_1(x, y)$. The function $F_1(x, y)$ is graphed in Figure 3. This is readily continued into the other quadrants through the symmetry requirements that it is odd in both x and y.

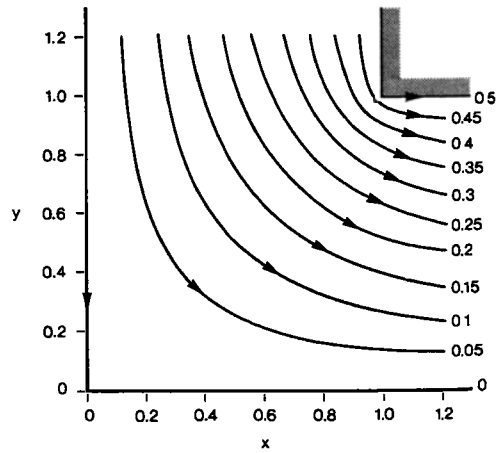

Fig. 3. Laplace flows. Canonical stream function $F_1(x, y)$ in the upper right quadrant. Curves with arrows are streamlines. Numerals on them are values of F_1.

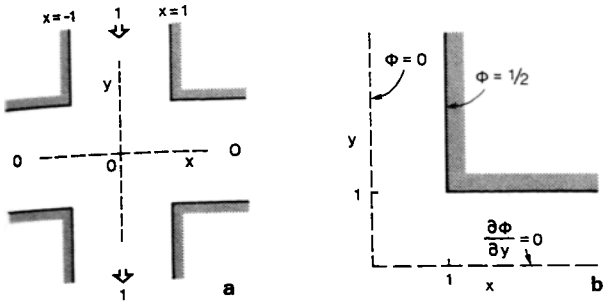

Fig. 4. (*a*) Discharge pattern (0, 0, 1). (*b*) Boundary conditions for the upper right quadrant.

4.3. *Discharge Pattern (0, 0, 1)*

The discharge pattern (0, 0, 1) is illustrated in Figure 4*a*. Note that the triads (0, 0, 1) and (0, 1, 0) describe continuous discharge patterns with $\Omega = 0$; accordingly, they are normalized, not with respect to Ω, but to b and a, respectively. We need solve (8) only in the quadrant $x \geq 0$, $y \geq 0$ subject to the boundary conditions

$$\Phi = 0 \qquad \text{on } x = 0$$
$$\Phi = \tfrac{1}{2} \qquad \text{on } x = 1,\ y \geq 1 \qquad x \geq 1,\ y = 1 \tag{11}$$
$$\partial\Phi/\partial y = 0 \qquad \text{on } y = 0$$

(See Figure 4*b*.)

The required solution is again found by conformal mapping (appendix), with parameter r ranging from 0 as $y \to \infty$ to $\frac{1}{2}\sin 2\pi\Phi \tan 2\pi\Phi$ on $y = 0$. It is similar in form to (10) except that in the expression for x_1 the term $4r^2 \cos^2 2\pi\Phi$ is replaced by $(\sin^2 2\pi\Phi - 2r \cos 2\pi\Phi)^2$, and in the expression for y_1 $r \cos 2\pi\Phi$ is replaced by $\frac{1}{2}\sin^2 2\pi\Phi - r \cos 2\pi\Phi$. The sign $\pm$ is taken according to the sign of $\frac{1}{2}\sin^2 2\pi\Phi - r \cos 2\pi\Phi$.

We denote the explicit form of this solution as $F_3(x, y)$, graphed in Figure 5. $F_3(x, y)$ is readily continued to other quadrants through the symmetry requirements that it is odd in x and even in y.

Rotating the pattern (0, 0, 1) through angle $-\frac{1}{2}\pi$ gives the pattern (0, 1, 0). The solution for pattern (0, 1, 0) is therefore

$$F_2(x, y) = F_3(y, -x) \tag{12}$$

It thus follows directly from the foregoing solution of (8) subject to (11).

4.4. *Superposing the Canonical Solutions*

The solution for the general discharge pattern (1, a, b) is therefore

$$\Phi(x, y) = F_1(x, y) + aF_2(x, y) + bF_3(x, y)$$
$$= F_1(x, y) + aF_3(y, -x) + bF_3(x, y) \tag{13}$$

5. STOKES FLOWS: APPROXIMATE SOLUTION

For Stokes flows through the junction, (6) satisfies the appropriate boundary conditions on (8), such as (9) and (10), together with the extra no-slip boundary condition that

$$\partial\Phi/\partial v = 0 \qquad \text{on all branch walls} \tag{14}$$

with $\partial/\partial v$ the normal derivative. Here we develop a simple approximate solution of (6) which satisfies all boundary conditions and is essentially exact for $|x|$ or $|y|$ greater than about 2.

We employ the approximation that for the canonical flows (1, 0, 0) and (0, 0, 1), the streamline patterns for Stokes flows are the same as those for Laplace flows, but that, in general, the stream function values Φ (for Laplace flow) and Φ_s (for Stokes flow) differ. The values of Φ_s are fixed by exactly matching the canonical flows at large x and y, so that

$$\Phi_s = \Phi(\tfrac{3}{2} - 2\Phi^2) \tag{15}$$

It is simply shown that (15) exactly satisfies all the boundary conditions on (6), including the no-slip condition (14).

Our canonical solutions for Stokes flows are then

$$F_{1s} = F_1(\tfrac{3}{2} - 2F_1^2) \qquad F_{2s} = F_2(\tfrac{3}{2} - 2F_2^2)$$
$$F_{3s} = F_3(\tfrac{3}{2} - 2F_3^2) \tag{16}$$

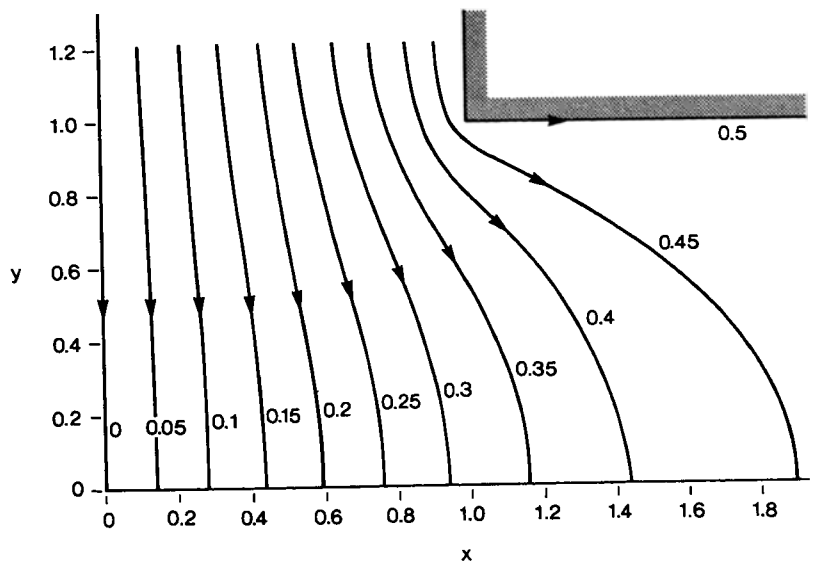

Fig. 5. Laplace flows. Canonical stream function $F_3(x, y)$ in the upper right quadrant. Numerals on the streamlines are values of F_3.

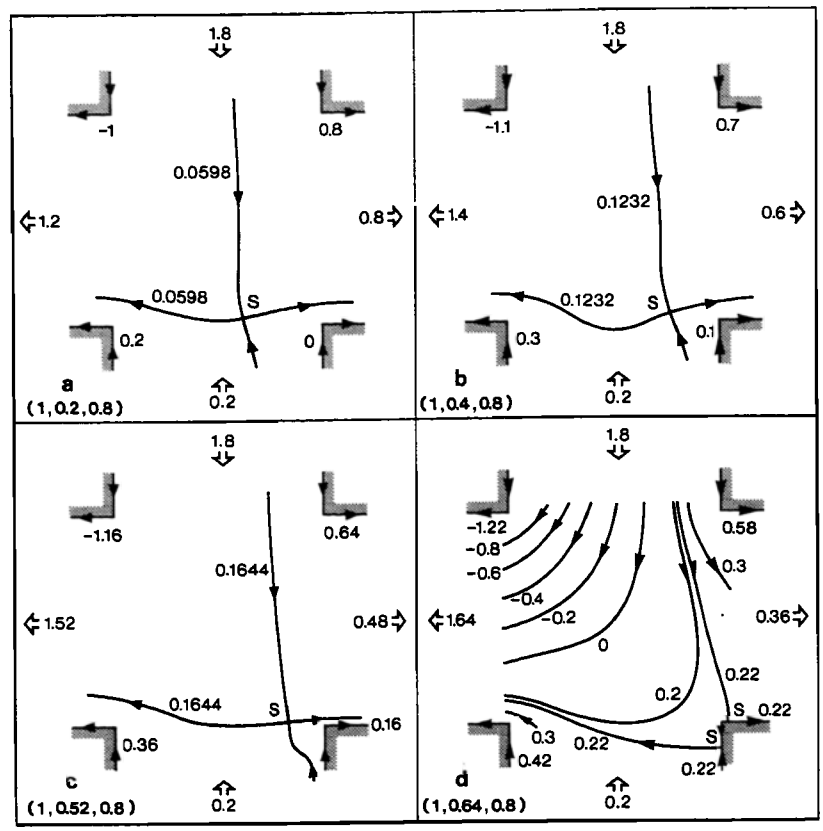

Fig. 6. Laplace flows. Dividing streamlines for the flow patterns: (*a*) (1, 0.2, 0.8), (*b*) (1, 0.4, 0.8), and (*c*) (1, 0.52, 0.8). Note how the stagnation point S moves toward the lower right corner as b increases from 0.2 to 0.52. (*d*) Detailed streamline plot for flow pattern (1, 0.64, 0.8). Dividing streamline is $\Phi = 0.22$. Note the two stagnation points S on lower right corner wall.

with the solution for the general discharge pattern (1, a, b) given by an equation similar to (13).

This approximation is certainly least accurate within the junction, but it is believed to be useful in a first demonstration of the difference in character between streamline routing for Laplace flows and Stokes flows.

6. Results for Laplace Flows

Solutions for various combinations of a and b in the range $0 \leq a, b < 1$ were simply calculated from the canonical solutions. Our principal concerns here are to establish the dividing streamline and to use it to test the validity of proportional routing.

6.1. *Dividing Streamline*

The dividing streamline is the streamline which divides each of inflows 2 and 4 into the part which goes into branch 1 and and that which goes into branch 3. When a and b are small enough, the dividing streamline defines a saddle point in Φ, which is, in fact, a stagnation point. (Note that the speculation of *Hull and Koslow* [1986] developed in their Figure 3 is not a "possible" flow: the only permissible turning point in Φ away from the channel walls is a saddle point, regardless of flow type.) When a and b are large enough, the dividing streamline assumes a different character: it contains one or two stagnation points located on channel walls.

Figure 6 illustrates the behavior of the dividing streamline. It is for discharge patterns with $b = 0.8$ and $a = 0.2$, 0.4, 0.52, and 0.64. Note how the stagnation point S moves toward the junction corner $(x, y) = (1, -1)$ as a increases. For $a \approx 0.566$ the stagnation point hits the wall just below this corner, and as a increases further the solitary stagnation point splits into two, with one stagnation point moving downwards along the wall $x = 1$, $y < -1$, and the other moving ultimately to the right along the wall $y = -1$, $x > 1$. (See Figure 6*d* for $a = 0.64$.)

6.2. *Outlet Solute Concentration*

With the dividing streamline established it is an elementary matter to compare results with those for proportional routing proposed by *Hull and Koslow* [1986]. It is pertinent to compare outlet solute concentrations for Laplace (and later Stokes) flows with those predicted by proportional routing. For definiteness (but with no loss of essential generality) we assume that inflow 4 has unit concentration of a particular solute, whereas inflow 2 has zero concentration. It is convenient to fix attention on C, the mean concentration in outflow branch 1 for Laplace (and later Stokes) flows. In due course we compare C with $\bar{C}$, the value according to proportional routing. The deviation of the ratio $C/\bar{C}$ from unity is evidently a measure of the error of proportional routing for the particular discharge pattern.

Basing our comparison thus on fractional concentration errors of the marker of the smaller inlet flow gives a stringent test of experiment and theory, oriented to the critical practical case of a small inlet flow of an undesirable pollutant. *Hull and*

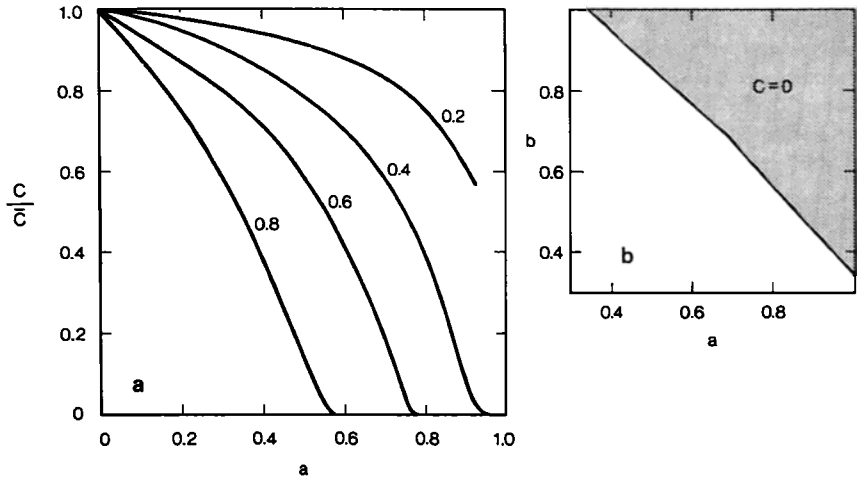

Fig. 7. Laplace flows. (*a*) Dependence of $C/\bar{C}$ on a and b. Numerals on the curves are values of b; $1 - C/\bar{C}$ is a measure of the error of proportional routing. (*b*) Map of the (a, b) plane. In the shaded area $C = 0$ and proportional routing is maximally incorrect.

Koslow [1986] reported their experiments in terms of KCl, the marker of the larger inlet flow. Outlet concentrations of KCl were large, so fractional concentration errors came out as small. Our more severe test looks at $KMnO_4$ concentrations (marker of the smaller inlet flows) in the Hull-Koslow experiments.

We note that the values of the stream function Φ at the lower left and right junction corners are $\frac{1}{2}(1 - a + b)$ and $\frac{1}{2}(-1 + a + b)$, respectively. It then follows that

$$C = \frac{\Phi_* - \frac{1}{2}(-1 + a + b)}{\frac{1}{2}(1 - a + b) - \frac{1}{2}(-1 + a + b)} = \frac{\Phi_* - \frac{1}{2}(-1 + a + b)}{1 - a} \qquad (17)$$

where $\Phi = \Phi_*$ is the dividing streamline for Laplace (and later Stokes) flows. We note in passing that with S the stagnation point(s) at the wall $\Phi_* = \frac{1}{2}(-1 + a + b)$, $C = 0$, and the whole of the solute entering by branch 2 leaves by branch 3.

6.3. *Implications of Proportional Routing*

On the other hand, proportional routing predicts that the dividing streamline $\Phi = \bar{\Phi}_*$ is such that

$$\bar{\Phi}_* = \tfrac{1}{2}(-1 + a + b) + \tfrac{1}{2}(1 - a)(1 - b) = \tfrac{1}{2}ab \qquad (18)$$

In general, $\bar{\Phi}_* \neq \Phi_*$, the value for Laplace (or Stokes) flows. Accordingly, in general, $\bar{C} \neq C$, and (17) is replaced for proportional routing by

$$\bar{C} = \frac{\frac{1}{2}ab - \frac{1}{2}(-1 + a + b)}{1 - a} = \tfrac{1}{2}(1 - b) \qquad (19)$$

It then follows from (17) and (19) that

$$\frac{C}{\bar{C}} = \frac{2\Phi_* + 1 - a - b}{(1 - a)(1 - b)} \qquad (20)$$

6.4. *Evaluation of $C/\bar{C}$: Test of Proportional Routing*

Figure 7*a* shows the dependence of $C/\bar{C}$ on a for $b = 0.2$, 0.4, 0.6, and 0.8; Figure 7*b* is a map of the (a, b) plane showing the region where $C/\bar{C} = 0$ and proportional routing is maximally incorrect. We leave further discussion of these results to sections 8 and 9 below.

7. Results for Stokes Flows

Figures 8 and 9 show the Stokes solutions for (1, 0, 0) and (0, 0, 1), respectively, found by the approximation of section 5. It is illuminating to compare these with the corresponding Laplace solutions (Figures 3 and 5). Note how the regions of largest flow velocity tend to occur in midstream for the Stokes flows, whereas they are at the junction corners for the Laplace flows.

Here also we used our canonical solutions to calculate solutions for various combinations of a and b. The results were qualitatively similar to those for Laplace flows. The stagnation points, however, tend to occur further from the walls than the corresponding Laplace stagnation points and the errors of proportional routing tend to be less. Figure 10 shows the

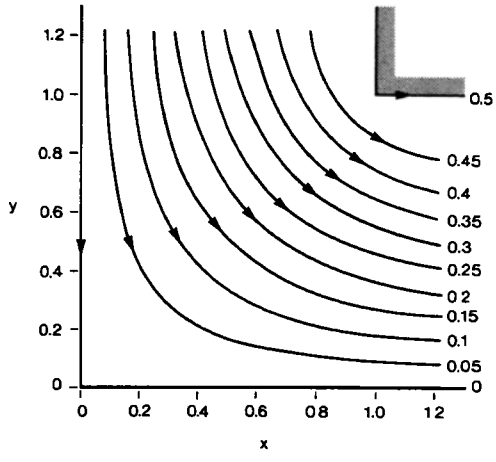

Fig. 8. Stokes flows. Approximation to the canonical stream function $F_{1s}(x, y)$ in the upper right quadrant. Numerals on the streamlines are values of F_{1s}. Note that the corresponding Laplace flow (Figure 3) tends to cut the corner $(x, y) = (1, 1)$, whereas this Stokes flow tends to avoid it.

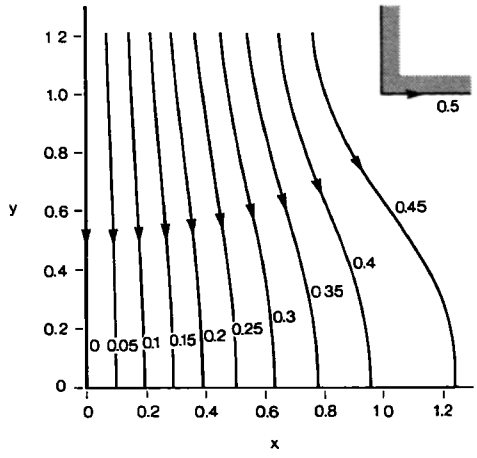

Fig. 9. Stokes flows. Approximation to the canonical stream function $F_{3s}(x, y)$ in the upper right quadrant. Numerals on the streamlines are values of F_{3s}. Note that the corresponding Laplace flow (Figure 5) tends to cut the corner $(x, y) = (1, 1)$, whereas this Stokes flow tends to avoid it.

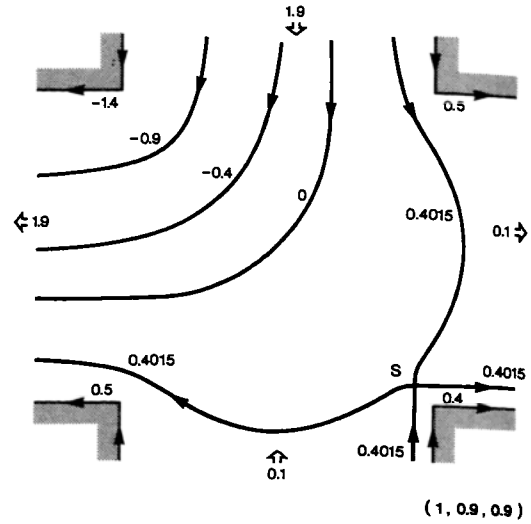

Fig. 10. Stokes flow. Detailed streamline plot for flow pattern (1, 0.9, 0.9). S is the stagnation point. Dividing streamline is $\Phi = 0.4015$. Plot is based on the approximation explained in section 5.

Stokes flow pattern (1, 0.9, 0.9). In this case $\Phi_* = 0.4015$, giving $C/\bar{C} = 0.30$.

Figure 11*a* shows the dependence of $C/\bar{C}$ on a for $b = 0.64$, 0.8, and 0.9; Figure 11*b* is a map of the (a, b) plane showing the region where $C/\bar{C} = 0$ and proportional routing is maximally incorrect. See the following sections for further discussion.

8. Experiments of Hull and Koslow [1986]: Critique of Proportional Routing

The foregoing analyses indicate that proportional routing is seriously in error when a and b are large enough. Here we compare our results for Laplace and Stokes flows with the experimental data of *Hull and Koslow* [1986]. Their tests F1-F5 are especially suited to the comparison, since they are for the largest b value, and for a range of a systematically increasing to the largest a value. These tests, like the others, involve errors of mass balance of both water (up to 7%) and of solute (up to 5%). We therefore calculated a and b from the equations

$$a = \frac{Q_{1\kappa} - Q_{4\kappa}}{Q_{1\kappa} + Q_{4\kappa}} \qquad b = \frac{Q_{2\kappa} - Q_{3\kappa}}{Q_{2\kappa} + Q_{3\kappa}}$$

with the suffix κ indicating the measured flows $Q_1, \cdots, Q_4$ of *Hull and Koslow*, retaining their numbering of branches, and we restored mass balance of solute (though not necessarily removed error) by making

$$1 - C = C_{4\kappa} \times \frac{\text{mean KC1 concentration in}}{\text{mean KC1 concentration out}}$$

$$= C_{4\kappa} \times \frac{Q_{2\kappa}}{Q_{2\kappa} + Q_{3\kappa}} \div \frac{Q_{1\kappa}C_{1\kappa} + Q_{4\kappa}C_{4\kappa}}{Q_{1\kappa} + Q_{4\kappa}}$$

Here $C_{4\kappa}$ denotes the Hull-Koslow measured C_4.

Table 1 shows the comparison for test series F. We reiterate that our C, $\bar{C}$ refer to concentrations of the solute which came

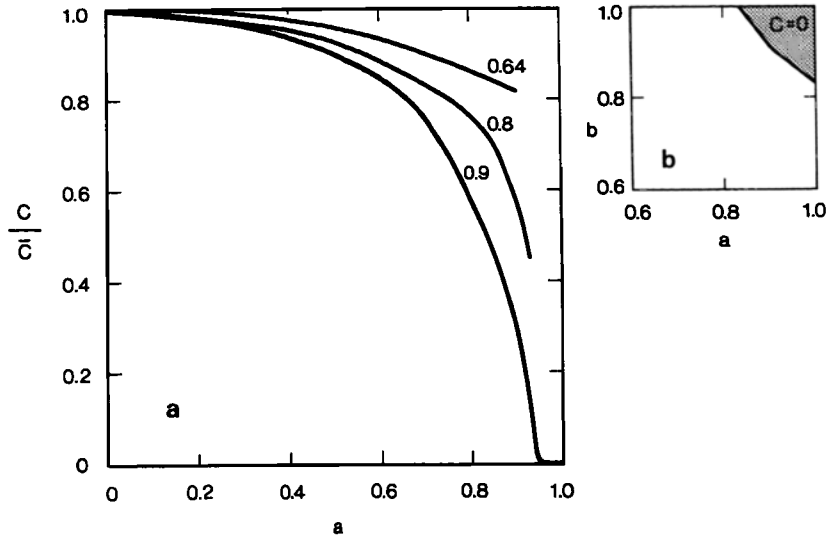

Fig. 11. Same as Figures 7*a* and 7*b*, but for Stokes flows. Results based on the approximation explained in section 5.

from the inlet with the smaller discharge. They thus apply to the $KMnO_4$ concentrations so that, for example, $\bar{C}$ in the table corresponds to the "calculated" values of $1 - C_1$ or $1 - C_4$ in Table 3*b* of *Hull and Koslow* [1986].

The final three columns of Table 1 compare the measured, Laplace, and Stokes values of $C/\bar{C}$. The measured values agree fairly well with the Laplace values. On the other hand, the Stokes values deviate only slightly from 1. We find, in fact, that the mean error of proportional routing, as indicated by $1 - C/\bar{C}$, has the measured value 0.647 and the Laplace value 0.612. The Stokes value, however, is only 0.034. We cannot explain why the experimental $C/\bar{C}$ values approximated the Laplace values and not the Stokes values.

One point must be made. *Hull and Koslow* [1986] claim "excellent agreement" between measured concentrations and those given by proportional routing. It is true that the errors of proportional routing are small for discharge patterns with a and b small (i.e., when the magnitudes of the branch discharges do not differ greatly); but not only our Laplace and Stokes analyses, but also Hull and Koslow's own data show that proportional routing fails increasingly badly as a and b increase. Oddly, one would have expected the Hull-Koslow experiments to reproduce Stokes flow conditions fairly closely and so to support proportional routing more strongly than they do.

9. Concluding Remarks

9.1. *Stokes Flows and Real-World Fracture Junctions*

Real-world fractures tend to be narrow and deep, and we should expect the flows to approximate Stokes flows rather than Laplace flows. We see from Figure 11 that for such flows, it is only when both a and b are greater than about 0.65 that the errors of proportional routing are likely to be of practical importance. The critical cases thus involve one large and one small inflow, and one large and one small outflow.

Consider a situation with one very small inflow with high solute concentration: then the fate of the solute downstream of the junction depends critically on the ratio of the outflow discharges. The solute will be partitioned evenly for equal discharges, but it will go wholly into one outlet if its discharge is large enough. Note that if there were scope for controlling the outlet discharges (e.g., by throttling or pumping) one could control the destination of the solute.

9.2. *Extensions of Analysis*

Finally, we point out that if desired, the present analysis can be extended to junctions of fractures of different widths, with different numbers of branches, and different angles of intersection of the branches. The Laplace solutions will generally depend on the appropriate conformal transformation (equation (21) in the present work). The required transformations are available through the well-known Schwarz-Christoffel formula [*Christoffel*, 1867; *Schwarz*, 1869].

TABLE 1. Comparison of Measurements of Hull and Koslow With Laplace and Stokes Flows

Test	a	b	$\bar{C}$	Measured C	$C/\bar{C}$		
					Measured	Laplace	Stokes
F1	0.105	0.578	0.211	0.188	0.891	0.94	1.00
F2	0.370	0.578	0.211	0.160	0.758	0.76	0.99
F3	0.452	0.578	0.211	0.141	0.668	0.66	0.98
F4	0.622	0.578	0.211	0.108	0.512	0.42	0.94
F5	0.684	0.578	0.211	0.086	0.408	0.28	0.92

Appendix: Laplace Canonical Solutions

Conformal Transformation

The conformal transformation [*Kober*, 1952, p. 157]

$$x + iy = z = \pi^{-1}[\cos^{-1} w + \cosh^{-1} w^{-1}] \tag{21}$$

transforms the real axis KNMLK and the lower half of the w plane ($w = s + it$) into the upper right quadrant of the flow field in the z plane (see Figure 12).

Solving for Discharge Pattern (1, 0, 0)

Boundary conditions (9) transform in the w plane to

$$\Phi = 0 \quad \text{on KLM} \qquad \Phi = \tfrac{1}{2} \quad \text{on MNK} \tag{22}$$

The solution of (8) and (22) is given implicitly by

$$s = r \cos 2\pi\Phi \qquad t = -r \sin 2\pi\Phi \qquad r = (s^2 + t^2)^{1/2} \tag{23}$$

Reverting to (21) we write

$$x + iy = (x_1 + x_2) + i(y_1 + y_2) \tag{24}$$

with

$$x_1 + iy_1 = \pi^{-1} \cos^{-1} w \qquad x_2 + iy_2 = \pi^{-1/2} \cosh^{-1} w^{-1}$$

Equations (23) then give

$$\cos \pi(x_1 + iy_1) = r(\cos 2\pi\Phi - i \sin 2\pi\Phi) \tag{25a}$$

$$\cosh \pi(x_2 + iy_2) = r^{-1}(\cos 2\pi\Phi + i \sin 2\pi\Phi) \tag{25b}$$

Manipulating (25*a*) to give x_1, y_1 explicitly gives (10*c*) and (10*d*) and manipulating (25*b*) yields

$$x_2 = \pi^{-1} \cosh^{-1}\left[\frac{\cosh \pi y_1}{r}\right] \qquad y_2 = \pi^{-1} \cos^{-1}\left[\frac{\cos \pi x_1}{r}\right] \tag{26}$$

Equations (10*a*) and (10*b*) follow at once.

Solving for Discharge Pattern (0, 0, 1)

Boundary conditions (11) transform in the w plane to

$$\Phi = 0 \quad \text{on KL} \quad \partial\Phi/\partial t = 0 \quad \text{on LM} \quad \Phi = \tfrac{1}{2} \quad \text{on MNK} \tag{27}$$

The solution of (8) and (27) [cf. *Moon and Spencer*, 1961, p. 17] is given implicitly by the family of confocal hyperbolae

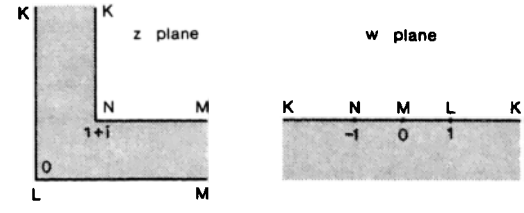

Fig. 12. Conformal transformation (21).

Φ = constant defined by

$$s = \tfrac{1}{2}[1 - \cosh \eta \cos 2\pi\Phi] \quad t = -\tfrac{1}{2} \sinh \eta \sin 2\pi\Phi. \quad (28)$$

Here η is the elliptic coordinate with $\eta = 0$, $0 \leq \Phi \leq \frac{1}{2}$, representing LM in the w plane, and

$$\cosh \eta = 2r - \cos 2\pi\Phi \quad (29)$$

Calculations similar to those for the previous flow problem then show that the solution in the z plane takes a form similar to (10) except for the differences noted in section 4.3.

Acknowledgment. I am grateful to L. C. Hull, Idaho National Engineering Laboratory, for helpful correspondence.

REFERENCES

Christoffel, E. B., Sul problema delle temperature stazionarie, e la rappresentazione di una data superficie, *Ann. Mat. Pura Appl.*, *1*, 89–103, 1867.

Hele-Shaw, H. J. S., The flow of water, *Nature*, *58*, 34–36, 1898.

Hull, L. C., and K. N. Koslow, Streamline routing through fracture junctions, *Water Resour. Res.*, *22*, 1731–1734, 1986.

Kober, H., *Dictionary of Conformal Representations*, 208 pp., Dover, Mineola, N. Y., 1952.

Moon, P., and D. E. Spencer, *Field Theory Handbook*, 236 pp., Springer, New York, 1961.

Schwarz, H. A., Ueber einige Abbildungsaufgaben, *Crelle's J. Math.*, *70*, 105–120, 1869.

Stokes, G. G., On the effect of the internal friction of fluids on the motion of pendulums, *Trans. Cambridge Philos. Soc.*, *9*, 8–106, 1851.

J. R. Philip, Division of Environmental Mechanics, CSIRO, GPO Box 821, Canberra, ACT 2601, Australia.

(Received February 23, 1987;
revised October 9, 1987;
accepted October 13, 1987.)